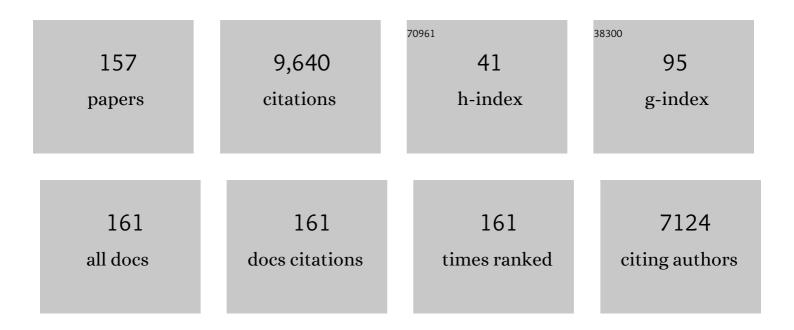
Grzegorz Greczynski

List of Publications by Year in descending order

Source: https://exaly.com/author-pdf/4740573/publications.pdf Version: 2024-02-01



#	Article	IF	CITATIONS
1	Morphology effects on electrocatalysis of anodic water splitting on nickel (II) oxide. Microporous and Mesoporous Materials, 2022, 333, 111734.	2.2	17
2	Dense, single-phase, hard, and stress-free Ti0.32Al0.63W0.05N films grown by magnetron sputtering with dramatically reduced energy consumption. Scientific Reports, 2022, 12, 2166.	1.6	8
3	Undressing the myth of apparent constant binding energy of the C 1 s peak from adventitious carbon in x-ray photoelectron spectroscopy. , 2022, 1, 100007.		8
4	Improving oxidation and wear resistance of TiB2 films by nano-multilayering with Cr. Surface and Coatings Technology, 2022, 436, 128337.	2.2	4
5	Nano-columnar, self-organised NiCrC/a-C:H thin films deposited by magnetron sputtering. Applied Surface Science, 2022, 591, 153134.	3.1	2
6	Microstructure, mechanical, and corrosion properties of Zr1-xCrxBy diboride alloy thin films grown by hybrid high power impulse/DC magnetron co-sputtering. Applied Surface Science, 2022, 591, 153164.	3.1	3
7	Thermal, electrical, and mechanical properties of hard nitrogen-alloyed Cr thin films deposited by magnetron sputtering. Surface and Coatings Technology, 2022, 441, 128575.	2.2	6
8	High-entropy transition metal nitride thin films alloyed with Al: Microstructure, phase composition and mechanical properties. Materials and Design, 2022, 219, 110798.	3.3	8
9	Reprint of: Improving oxidation and wear resistance of TiB2 films by nano-multilayering with Cr. Surface and Coatings Technology, 2022, 442, 128602.	2.2	2
10	Domain epitaxial growth of Ta3N5 film on c-plane sapphire substrate. Surface and Coatings Technology, 2022, 443, 128581.	2.2	4
11	A step-by-step guide to perform x-ray photoelectron spectroscopy. Journal of Applied Physics, 2022, 132,	1.1	141
12	Oxidation kinetics of overstoichiometric TiB2 thin films grown by DC magnetron sputtering. Corrosion Science, 2022, 206, 110493.	3.0	17
13	Age hardening in superhard ZrB2-rich Zr1-xTaxBy thin films. Scripta Materialia, 2021, 191, 120-125.	2.6	28
14	Towards reliable X-ray photoelectron spectroscopy: Sputter-damage effects in transition metal borides, carbides, nitrides, and oxides. Applied Surface Science, 2021, 542, 148599.	3.1	110
15	Multifunctional ZrB2-rich Zr1-xCrxBy thin films with enhanced mechanical, oxidation, and corrosion properties. Vacuum, 2021, 185, 109990.	1.6	21
16	Orthorhombic Ta3-xN5-yOy thin films grown by unbalanced magnetron sputtering: The role of oxygen on structure, composition, and optical properties. Surface and Coatings Technology, 2021, 406, 126665.	2.2	5
17	Phase Transformation and Superstructure Formation in (Ti0.5, Mg0.5)N Thin Films through High-Temperature Annealing. Coatings, 2021, 11, 89.	1.2	2
		c .	

¹⁸ X-ray photoelectron spectroscopy analysis of TiBx (1.3 â‰â€‰x â‰â€‰3.0) thin films. Journal of Vacuum, Science 7 and Technology A: Vacuum, Surfaces and Films, 2021, 39, .

#	Article	IF	CITATIONS
19	Dense Ti0.67Hf0.33B1.7 thin films grown by hybrid HfB2-HiPIMS/TiB2-DCMS co-sputtering without external heating. Vacuum, 2021, 186, 110057.	1.6	9
20	ZrCuAlNi thin film metallic glass grown by high power impulse and direct current magnetron sputtering. Surface and Coatings Technology, 2021, 412, 127029.	2.2	13
21	Phase formation and structural evolution of multicomponent (CrFeCo)1-yNy films. Surface and Coatings Technology, 2021, 412, 127059.	2.2	5
22	The same chemical state of carbon gives rise to two peaks in X-ray photoelectron spectroscopy. Scientific Reports, 2021, 11, 11195.	1.6	353
23	Preparation and tunable optical properties of amorphous AlSiO thin films. Vacuum, 2021, 187, 110074.	1.6	4
24	Toward energy-efficient physical vapor deposition: Routes for replacing substrate heating during magnetron sputter deposition by employing metal ion irradiation. Surface and Coatings Technology, 2021, 415, 127120.	2.2	23
25	Improved oxidation properties from a reduced B content in sputter-deposited TiBx thin films. Surface and Coatings Technology, 2021, 420, 127353.	2.2	24
26	Influence of Si content on phase stability and mechanical properties of TiAlSiN films grown by AlSi-HiPIMS/Ti-DCMS co-sputtering. Surface and Coatings Technology, 2021, 427, 127661.	2.2	22
27	Study of Cucurbit[7]uril nanocoating on epitaxial graphene to design a versatile sensing platform. Applied Surface Science, 2021, 563, 150096.	3.1	2
28	Towards energy-efficient physical vapor deposition: Mapping out the effects of W+ energy and concentration on the densification of TiAlWN thin films grown with no external heating. Surface and Coatings Technology, 2021, 424, 127639.	2.2	15
29	Systematic compositional analysis of sputter-deposited boron-containing thin films. Journal of Vacuum Science and Technology A: Vacuum, Surfaces and Films, 2021, 39, .	0.9	26
30	Thermally induced structural evolution and age-hardening of polycrystalline V1–xMoxN (xÂâ‰^Â0.4) thin films. Surface and Coatings Technology, 2021, 405, 126723.	2.2	11
31	X-ray photoelectron spectroscopy: Towards reliable binding energy referencing. Progress in Materials Science, 2020, 107, 100591.	16.0	1,284
32	Surface functionalization of epitaxial graphene using ion implantation for sensing and optical applications. Carbon, 2020, 157, 169-184.	5.4	15
33	Cubic-structure Al-rich TiAlSiN thin films grown by hybrid high-power impulse magnetron co-sputtering with synchronized Al+ irradiation. Surface and Coatings Technology, 2020, 385, 125364.	2.2	10
34	Effect of nitrogen content on microstructure and corrosion resistance of sputter-deposited multicomponent (TiNbZrTa)Nx films. Surface and Coatings Technology, 2020, 404, 126485.	2.2	16
35	Improving the high-temperature oxidation resistance of TiB2 thin films by alloying with Al. Acta Materialia, 2020, 196, 677-689.	3.8	65
36	Self-organized columnar Zr0.7Ta0.3B1.5 core/shell-nanostructure thin films. Surface and Coatings Technology, 2020, 401, 126237.	2.2	15

#	Article	IF	CITATIONS
37	Cobalt thin films as water-recombination electrocatalysts. Surface and Coatings Technology, 2020, 404, 126643.	2.2	8
38	XPS guide: Charge neutralization and binding energy referencing for insulating samples. Journal of Vacuum Science and Technology A: Vacuum, Surfaces and Films, 2020, 38, .	0.9	114
39	Electronic excitation of transition metal nitrides by light ions with keV energies. Journal of Physics Condensed Matter, 2020, 32, 405502.	0.7	1
40	Metal-ion subplantation: A game changer for controlling nanostructure and phase formation during film growth by physical vapor deposition. Journal of Applied Physics, 2020, 127, .	1.1	30
41	Oxidation behaviour of V2AlC MAX phase coatings. Journal of the European Ceramic Society, 2020, 40, 4436-4444.	2.8	33
42	High Si content TiSiN films with superior oxidation resistance. Surface and Coatings Technology, 2020, 398, 126087.	2.2	30
43	Microstructure and mechanical, electrical, and electrochemical properties of sputter-deposited multicomponent (TiNbZrTa)Nx coatings. Surface and Coatings Technology, 2020, 389, 125651.	2.2	37
44	Structural Modifications in Epitaxial Graphene on SiC Following 10 keV Nitrogen Ion Implantation. Applied Sciences (Switzerland), 2020, 10, 4013.	1.3	7
45	Growth of dense, hard yet low-stress Ti0.40Al0.27W0.33N nanocomposite films with rotating substrate and no external substrate heating. Journal of Vacuum Science and Technology A: Vacuum, Surfaces and Films, 2020, 38, .	0.9	13
46	Compromising Science by Ignorant Instrument Calibration—Need to Revisit Half a Century of Published XPS Data. Angewandte Chemie, 2020, 132, 5034-5038.	1.6	143
47	Compromising Science by Ignorant Instrument Calibration—Need to Revisit Half a Century of Published XPS Data. Angewandte Chemie - International Edition, 2020, 59, 5002-5006.	7.2	429
48	Structural and mechanical properties of amorphous AlMgB14 thin films deposited by DC magnetron sputtering on Si, Al2O3 and MgO substrates. Applied Physics A: Materials Science and Processing, 2020, 126, 1.	1.1	5
49	X-ray photoelectron spectroscopy studies of Ti1-Al N (0 â‰≇€¯x â‰≇€¯0.83) high-temperature oxidation: Th crucial role of Al concentration. Surface and Coatings Technology, 2019, 374, 923-934.	1e 2.2	64
50	Reactive magnetron sputtering of tungsten target in krypton/trimethylboron atmosphere. Thin Solid Films, 2019, 688, 137384.	0.8	6
51	A simple model for non-saturated reactive sputtering processes. Thin Solid Films, 2019, 688, 137413.	0.8	10
52	Paradigm shift in thin-film growth by magnetron sputtering: From gas-ion to metal-ion irradiation of the growing film. Journal of Vacuum Science and Technology A: Vacuum, Surfaces and Films, 2019, 37, .	0.9	94
53	Quasi-amorphous, nanostructural CoCrMoC/a-C:H coatings deposited by reactive magnetron sputtering. Surface and Coatings Technology, 2019, 378, 124910.	2.2	7
54	Compositional dependence of epitaxial Tin+1SiCn MAX-phase thin films grown from a Ti3SiC2 compound target. Journal of Vacuum Science and Technology A: Vacuum, Surfaces and Films, 2019, 37, .	0.9	8

#	Article	IF	CITATIONS
55	Strategy for simultaneously increasing both hardness and toughness in ZrB2-rich Zr1â^'xTaxBy thin films. Journal of Vacuum Science and Technology A: Vacuum, Surfaces and Films, 2019, 37, .	0.9	42
56	Control over the Phase Formation in Metastable Transition Metal Nitride Thin Films by Tuning the Al+ Subplantation Depth. Coatings, 2019, 9, 17.	1.2	19
57	Corrosion Resistant TiTaN and TiTaAlN Thin Films Grown by Hybrid HiPIMS/DCMS Using Synchronized Pulsed Substrate Bias with No External Substrate Heating. Coatings, 2019, 9, 841.	1.2	5
58	Influence of Si doping and O2 flow on arc-deposited (Al,Cr)2O3 coatings. Journal of Vacuum Science and Technology A: Vacuum, Surfaces and Films, 2019, 37, 061516.	0.9	3
59	Electronic structure of β-Ta films from X-ray photoelectron spectroscopy and first-principles calculations. Applied Surface Science, 2019, 470, 607-612.	3.1	20
60	Effect of impurities on morphology, growth mode, and thermoelectric properties of (1 1 1) and (0 0 epitaxial-like ScN films. Journal Physics D: Applied Physics, 2019, 52, 035302.	1) 1.3	31
61	Synthesis and characterization of single-phase epitaxial Cr2N thin films by reactive magnetron sputtering. Journal of Materials Science, 2019, 54, 1434-1442.	1.7	16
62	Time evolution of ion fluxes incident at the substrate plane during reactive high-power impulse magnetron sputtering of groups IVb and VIb transition metals in Ar/N2. Journal of Vacuum Science and Technology A: Vacuum, Surfaces and Films, 2018, 36, .	0.9	31
63	Substantial difference in target surface chemistry between reactive dc and high power impulse magnetron sputtering. Journal Physics D: Applied Physics, 2018, 51, 05LT01.	1.3	10
64	Reliable determination of chemical state in x-ray photoelectron spectroscopy based on sample-work-function referencing to adventitious carbon: Resolving the myth of apparent constant binding energy of the C 1s peak. Applied Surface Science, 2018, 451, 99-103.	3.1	821
65	Controlling the B/Ti ratio of TiBx thin films grown by high-power impulse magnetron sputtering. Journal of Vacuum Science and Technology A: Vacuum, Surfaces and Films, 2018, 36, .	0.9	46
66	Enhanced Ti0.84Ta0.16N diffusion barriers, grown by a hybrid sputtering technique with no substrate heating, between Si(001) wafers and Cu overlayers. Scientific Reports, 2018, 8, 5360.	1.6	25
67	Chemical bonding in epitaxial ZrB2 studied by X-ray spectroscopy. Thin Solid Films, 2018, 649, 89-96.	0.8	20
68	Functionalization of bacterial cellulose wound dressings with the antimicrobial peptide <i>ε</i> -poly-L-Lysine. Biomedical Materials (Bristol), 2018, 13, 025014.	1.7	86
69	Reference binding energies of transition metal carbides by core-level x-ray photoelectron spectroscopy free from Ar+ etching artefacts. Applied Surface Science, 2018, 436, 102-110.	3.1	68
70	Highly Stable and Efficient Ligninâ€₽EDOT/PSS Composites for Removal of Toxic Metals. Advanced Sustainable Systems, 2018, 2, 1700114.	2.7	19
71	Modifications in structural, optical and electrical properties of epitaxial graphene on SiC due to 100 MeV silver ion irradiation. Materials Science in Semiconductor Processing, 2018, 74, 122-128.	1.9	10
72	Effect of ion-implantation-induced defects and Mg dopants on the thermoelectric properties of ScN. Physical Review B, 2018, 98, .	1.1	31

#	Article	IF	CITATIONS
73	Self-structuring in Zr1â^'xAlxN films as a function of composition and growth temperature. Scientific Reports, 2018, 8, 16327.	1.6	9
74	Electrical resistivity modulation of thermoelectric iron based nanocomposites. Vacuum, 2018, 157, 384-390.	1.6	3
75	Exploring NiO nanosize structures for ammonia sensing. Journal of Materials Science: Materials in Electronics, 2018, 29, 11870-11877.	1.1	19
76	V0.5Mo0.5Nx/MgO(001): Composition, nanostructure, and mechanical properties as a function of film growth temperature. Acta Materialia, 2017, 126, 194-201.	3.8	23
77	Unprecedented Al supersaturation in single-phase rock salt structure VAIN films by Al+ subplantation. Journal of Applied Physics, 2017, 121, .	1.1	40
78	Controlling the boron-to-titanium ratio in magnetron-sputter-deposited TiBx thin films. Journal of Vacuum Science and Technology A: Vacuum, Surfaces and Films, 2017, 35, .	0.9	40
79	Rolling performance of carbon nitride-coated bearing components in different lubrication regimes. Tribology International, 2017, 114, 141-151.	3.0	22
80	C 1s Peak of Adventitious Carbon Aligns to the Vacuum Level: Dire Consequences for Material's Bonding Assignment by Photoelectron Spectroscopy. ChemPhysChem, 2017, 18, 1507-1512.	1.0	695
81	Low-temperature growth of dense and hard Ti0.41Al0.51Ta0.08N films via hybrid HIPIMS/DC magnetron co-sputtering with synchronized metal-ion irradiation. Journal of Applied Physics, 2017, 121, .	1.1	28
82	Comparative study of macro- and microtribological properties of carbon nitride thin films deposited by HiPIMS. Wear, 2017, 370-371, 1-8.	1.5	11
83	Control of the metal/gas ion ratio incident at the substrate plane during high-power impulse magnetron sputtering of transition metals in Ar. Thin Solid Films, 2017, 642, 36-40.	0.8	24
84	Gas rarefaction effects during high power pulsed magnetron sputtering of groups IVb and VIb transition metals in Ar. Journal of Vacuum Science and Technology A: Vacuum, Surfaces and Films, 2017, 35, .	0.9	27
85	Native target chemistry during reactive dc magnetron sputtering studied by <i>ex-situ x</i> -ray photoelectron spectroscopy. Applied Physics Letters, 2017, 111, .	1.5	10
86	Ti ₂ Au ₂ C and Ti ₃ Au ₂ C ₂ formed by solid state reaction of gold with Ti ₂ AlC and Ti ₃ AlC ₂ . Chemical Communications, 2017, 53, 9554-9557.	2.2	53
87	ICMCTF 2017 $\hat{a} \in \hat{a}$ Preface. Surface and Coatings Technology, 2017, 332, 1.	2.2	0
88	Extended metastable Al solubility in cubic VAlN by metal-ion bombardment during pulsed magnetron sputtering: film stress <i>vs</i> subplantation. Journal of Applied Physics, 2017, 122, .	1.1	19
89	Core-level spectra and binding energies of transition metal nitrides by non-destructive x-ray photoelectron spectroscopy through capping layers. Applied Surface Science, 2017, 396, 347-358.	3.1	109
90	Selectable phase formation in VAIN thin films by controlling Al+ subplantation depth. Scientific Reports, 2017, 7, 17544.	1.6	18

#	Article	IF	CITATIONS
91	Impact of B_4C co-sputtering on structure and optical performance of Cr/Sc multilayer X-ray mirrors. Optics Express, 2017, 25, 18274.	1.7	15
92	Improved adhesion of carbon nitride coatings on steel substrates using metal HiPIMS pretreatments. Surface and Coatings Technology, 2016, 302, 454-462.	2.2	37
93	Venting temperature determines surface chemistry of magnetron sputtered TiN films. Applied Physics Letters, 2016, 108, .	1.5	92
94	<i>In-situ</i> observation of self-cleansing phenomena during ultra-high vacuum anneal of transition metal nitride thin films: Prospects for non-destructive photoelectron spectroscopy. Applied Physics Letters, 2016, 109, .	1.5	26
95	TiN diffusion barrier failure by the formation of Cu3Si investigated by electron microscopy and atom probe tomography. Journal of Vacuum Science and Technology B:Nanotechnology and Microelectronics, 2016, 34, .	0.6	13
96	Theoretical and experimental study of metastable solid solutions and phase stability within the immiscible Ag-Mo binary system. Journal of Applied Physics, 2016, 119, .	1.1	14
97	Nitrogen-doped bcc-Cr films: Combining ceramic hardness with metallic toughness and conductivity. Scripta Materialia, 2016, 122, 40-44.	2.6	41
98	Rolling contact fatigue of bearing components coated with carbon nitride thin films. Tribology International, 2016, 98, 100-107.	3.0	21
99	Self-consistent modelling of X-ray photoelectron spectra from air-exposed polycrystalline TiN thin films. Applied Surface Science, 2016, 387, 294-300.	3.1	131
100	Unintentional carbide formation evidenced during high-vacuum magnetron sputtering of transition metal nitride thin films. Applied Surface Science, 2016, 385, 356-359.	3.1	25
101	Novel transparent MgSiON thin films with high hardness and refractive index. Vacuum, 2016, 131, 1-4.	1.6	16
102	A comparative study of direct current magnetron sputtering and high power impulse magnetron sputtering processes for CNx thin film growth with different inert gases. Diamond and Related Materials, 2016, 64, 13-26.	1.8	20
103	Peak amplitude of target current determines deposition rate loss during high power pulsed magnetron sputtering. Vacuum, 2016, 124, 1-4.	1.6	51
104	Synthesis and characterization of Zr2Al3C4 thin films. Thin Solid Films, 2015, 595, 142-147.	0.8	10
105	Stability of 10B4C thin films under neutron radiation. Radiation Physics and Chemistry, 2015, 113, 14-19.	1.4	53
106	Novel hard, tough HfAlSiN multilayers, defined by alternating Si bond structure, deposited using modulated high-flux, low-energy ion irradiation of the growing film. Journal of Vacuum Science and Technology A: Vacuum, Surfaces and Films, 2015, 33, .	0.9	7
107	Strategy for tuning the average charge state of metal ions incident at the growing film during HIPIMS deposition. Vacuum, 2015, 116, 36-41.	1.6	34
108	Al capping layers for nondestructive x-ray photoelectron spectroscopy analyses of transition-metal nitride thin films. Journal of Vacuum Science and Technology A: Vacuum, Surfaces and Films, 2015, 33, .	0.9	33

#	Article	IF	CITATIONS
109	Control of Ti1â^'xSixN nanostructure via tunable metal-ion momentum transfer during HIPIMS/DCMS co-deposition. Surface and Coatings Technology, 2015, 280, 174-184.	2.2	53
110	Stoichiometric, epitaxial ZrB2 thin films with low oxygen-content deposited by magnetron sputtering from a compound target: Effects of deposition temperature and sputtering power. Journal of Crystal Growth, 2015, 430, 55-62.	0.7	33
111	Low-temperature growth of low friction wear-resistant amorphous carbon nitride thin films by mid-frequency, high power impulse, and direct current magnetron sputtering. Journal of Vacuum Science and Technology A: Vacuum, Surfaces and Films, 2015, 33, .	0.9	17
112	Growth and properties of amorphous Ti–B–Si–N thin films deposited by hybrid HIPIMS/DC-magnetron co-sputtering from TiB2 and Si targets. Surface and Coatings Technology, 2014, 259, 442-447.	2.2	11
113	Novel strategy for low-temperature, high-rate growth of dense, hard, and stress-free refractory ceramic thin films. Journal of Vacuum Science and Technology A: Vacuum, Surfaces and Films, 2014, 32, .	0.9	45
114	A review of metal-ion-flux-controlled growth of metastable TiAlN by HIPIMS/DCMS co-sputtering. Surface and Coatings Technology, 2014, 257, 15-25.	2.2	126
115	Strain-free, single-phase metastable Ti0.38Al0.62N alloys with high hardness: metal-ion energy vs. momentum effects during film growth by hybrid high-power pulsed/dc magnetron cosputtering. Thin Solid Films, 2014, 556, 87-98.	0.8	69
116	X-ray Photoelectron Spectroscopy Analyses of the Electronic Structure of Polycrystalline Ti1-xAlxN Thin Films with 0 â‰ û €‰x â‰ û €‰0.96. Surface Science Spectra, 2014, 21, 35-49.	0.3	20
117	Influence of inert gases on the reactive high power pulsed magnetron sputtering process of carbon-nitride thin films. Journal of Vacuum Science and Technology A: Vacuum, Surfaces and Films, 2013, 31, .	0.9	18
118	Reactive high power impulse magnetron sputtering of CFx thin films in mixed Ar/CF4 and Ar/C4F8 discharges. Thin Solid Films, 2013, 542, 21-30.	0.8	17
119	Effect of substrate temperature on properties of diamond-like films deposited by combined DC impulse vacuum-arc method. Surface and Coatings Technology, 2013, 236, 444-449.	2.2	28
120	Influence of Ti–Si cathode grain size on the cathodic arc process and resulting Ti–Si–N coatings. Surface and Coatings Technology, 2013, 235, 637-647.	2.2	16
121	Sputter-cleaned Epitaxial VxMo(1-x)Ny/MgO(001) Thin Films Analyzed by X-ray Photoelectron Spectroscopy: 3. Polycrystalline V0.49Mo0.51N1.02. Surface Science Spectra, 2013, 20, 80-85.	0.3	8
122	Sputter-cleaned Epitaxial VxMo(1-x)Ny/MgO(001) Thin Films Analyzed by X-ray Photoelectron Spectroscopy: 1. Single-crystal V0.48Mo0.52N0.64. Surface Science Spectra, 2013, 20, 68-73.	0.3	12
123	Sputter-cleaned Epitaxial VxMo(1-x)Ny/MgO(001) Thin Films Analyzed by X-ray Photoelectron Spectroscopy: 2. Single-crystal V0.47Mo0.53N0.92. Surface Science Spectra, 2013, 20, 74-79.	0.3	11
124	Structural and mechanical properties of Cr–Al–O–N thin films grown by cathodic arc deposition. Acta Materialia, 2012, 60, 6494-6507.	3.8	65
125	Metal versus rare-gas ion irradiation during Ti1â^'‹i›x‹/i›Al‹i›x‹/i›N film growth by hybrid high power pulsed magnetron/dc magnetron co-sputtering using synchronized pulsed substrate bias. Journal of Vacuum Science and Technology A: Vacuum, Surfaces and Films, 2012, 30, .	0.9	98
126	Ion mass spectrometry investigations of the discharge during reactive high power pulsed and direct current magnetron sputtering of carbon in Ar and Ar/N2. Journal of Applied Physics, 2012, 112, .	1.1	36

#	Article	IF	CITATIONS
127	Role of Tin+ and Aln+ ion irradiation (n=1, 2) during Ti1-xAlxN alloy film growth in a hybrid HIPIMS/magnetron mode. Surface and Coatings Technology, 2012, 206, 4202-4211.	2.2	119
128	Selection of metal ion irradiation for controlling Ti1â^'xAlxN alloy growth via hybrid HIPIMS/magnetron co-sputtering. Vacuum, 2012, 86, 1036-1040.	1.6	66
129	Ti–Si–C–N thin films grown by reactive arc evaporation from Ti ₃ SiC ₂ cathodes. Journal of Materials Research, 2011, 26, 874-881.	1.2	19
130	CFx thin solid films deposited by high power impulse magnetron sputtering: Synthesis and characterization. Surface and Coatings Technology, 2011, 206, 646-653.	2.2	43
131	Mitigating the geometrical limitations of conventional sputtering by controlling the ion-to-neutral ratio during high power pulsed magnetron sputtering. Thin Solid Films, 2011, 519, 6354-6361.	0.8	48
132	Microstructure evolution of Ti3SiC2 compound cathodes during reactive cathodic arc evaporation. Journal of Vacuum Science and Technology A: Vacuum, Surfaces and Films, 2011, 29, 031601.	0.9	10
133	Industrial-scale deposition of highly adherent CNx films on steel substrates. Surface and Coatings Technology, 2010, 204, 3349-3357.	2.2	33
134	Microstructure control of CrNx films during high power impulse magnetron sputtering. Surface and Coatings Technology, 2010, 205, 118-130.	2.2	77
135	Time and energy resolved ion mass spectroscopy studies of the ion flux during high power pulsed magnetron sputtering of Cr in Ar and Ar/N2 atmospheres. Vacuum, 2010, 84, 1159-1170.	1.6	116
136	\$hbox{CrN}_{m x}\$ Films Prepared by DC Magnetron Sputtering and High-Power Pulsed Magnetron Sputtering: A Comparative Study. IEEE Transactions on Plasma Science, 2010, 38, 3046-3056.	0.6	72
137	Joint Theoretical and Experimental Characterization of the Structural and Electronic Properties of Poly(dioctylfluorene-alt-N-butylphenyl diphenylamine). Journal of Physical Chemistry B, 2004, 108, 5594-5599.	1.2	38
138	The effects of solvents on the morphology and sheet resistance in poly(3,4-ethylenedioxythiophene)–polystyrenesulfonic acid (PEDOT–PSS) films. Synthetic Metals, 2003, 139, 1-10.	2.1	702
139	Electronic structure of poly(9,9-dioctylfluorene) in the pristine and reduced state. Journal of Chemical Physics, 2002, 116, 1700-1706.	1.2	25
140	Hybrid interfaces in polymer-based electronics. Synthetic Metals, 2001, 121, 1625-1628.	2.1	10
141	Energy level alignment at polymer/electrode interfaces in light-emitting devices studied by photoelectron spectroscopy. , 2001, , .		1
142	Photoelectron spectroscopy of thin films of PEDOT–PSS conjugated polymer blend: a mini-review and some new results. Journal of Electron Spectroscopy and Related Phenomena, 2001, 121, 1-17.	0.8	389
143	An experimental study of poly(9,9-dioctyl-fluorene) and its interfaces with Al, LiF and CsF. Applied Surface Science, 2001, 175-176, 319-325.	3.1	14
144	The electronic structure of polymer–metal interfaces studied by ultraviolet photoelectron spectroscopy. Materials Science and Engineering Reports, 2001, 34, 121-146.	14.8	84

#	Article	IF	CITATIONS
145	Photoelectron spectroscopy study of the energy level alignment at polymer/electrode interfaces in light emitting devices. Current Applied Physics, 2001, 1, 98-106.	1.1	10
146	Hybrid interfaces of poly(9,9-dioctylfluorene) employing thin insulating layers of CsF: A photoelectron spectroscopy study. Journal of Chemical Physics, 2001, 114, 8628-8636.	1.2	32
147	Electronic structure of pristine and sodium doped poly(p-pyridine). Journal of Chemical Physics, 2001, 114, 4243-4252.	1.2	12
148	Photoelectron spectroscopy of hybrid interfaces for light emitting diodes: Influence of the substrate work function. Applied Physics Letters, 2001, 79, 3185-3187.	1.5	7
149	Photoelectron Spectroscopy of Interfaces for Polymer-Based Electronic Devices. , 2001, , .		1
150	Thin Interfacial Layers in Polymer-Based Electronics. Materials Research Society Symposia Proceedings, 2000, 660, .	0.1	0
151	Electronic structure of hybrid interfaces of poly(9,9-dioctylfluorene). Chemical Physics Letters, 2000, 321, 379-384.	1.2	40
152	Polymer interfaces studied by photoelectron spectroscopy: Li on polydioctylfluorene and Alq3. Thin Solid Films, 2000, 363, 322-326.	0.8	26
153	An experimental study of poly(9,9-dioctyl-fluorene) and its interface with Li and LiF Applied Surface Science, 2000, 166, 380-386.	3.1	16
154	Thin Interfacial Layers in Polymer-Based Electronics. Materials Research Society Symposia Proceedings, 2000, 660, 1.	0.1	0
155	Energy level alignment in organic-based three-layer structures studied by photoelectron spectroscopy. Journal of Applied Physics, 2000, 88, 7187-7191.	1.1	28
156	An experimental study of poly(9,9-dioctyl-fluorene) and its interfaces with Li, Al, and LiF. Journal of Chemical Physics, 2000, 113, 2407-2412.	1.2	89
157	Characterization of the PEDOT-PSS system by means of X-ray and ultraviolet photoelectron spectroscopy. Thin Solid Films, 1999, 354, 129-135.	0.8	390